EasyChair Preprint

№ 9094

The Flight and Hovering of a Balloon-Multicopter with a Special Assembly Scheme Under Lateral Wind Disturbance

Duy Duyen Tran, Duc Cuong Nguyen and Viet Hung Nguyen

October 24, 2022

The flight and hovering of a balloon-multicopter with a special assembly scheme under lateral wind disturbance

Tran Duy Duyen[1], Nguyen Duc Cuong[2,*] và Nguyen Viet Hung[1]
[1] *Air Defense – Air Force Academy, Hanoi, Vietnam*
[2]*Vietnam Aerospace Association (VASA), Hanoi, Vietnam*
*Email: cuongnd45@gmail.com

ABSTRACT. The balloon-multicopter or ballooncopter is a new flight vehicle type that combines the advantages of a and those of a multicopter/ multirotor device G position when hovering and s). The ballooncopters can be highly effective in different fields such as monitoring, tourism and transportation to the areas that are difficult to reach. This article deals with ballooncopters that have a special solution to assemble a multicopter with the balloon and payload as a scheme of two seriesly hung pendulums. The assembly scheme many times reduces the necessary power of the rotors when needed to tilt the thrust vector. This new assembly scheme requires balance and stability considerations when flying in windy conditions. The longitudinal motion was considered in a paper of Aeronautical Journal (UK) that is to be published in near future. This article will deal with these problems in the scope of the action of lateral wind. To confirm the dynamic stability the authors use numerical testing in different wind disturbance. The motion of the ballooncopter is modeled using a 3-body, 6-degree-of-freedom mechanical system and the motion law of the system is determined by the method of Lagrange II equations; the calculation is done in MAPLE. The software was accurately verified when used as a design aid tool (CAE-Computer-Aided Engineering). The numerical testing results confirm the balance and stability of a hypothetical ballooncopter in the presence of lateral wind in a step form of disturbance at hovering flight with an autopilot and in a rectilinear flight. The numerical testing also show that the small oscillations may be damped by friction of the cardan joint for payload. In this case one can obtain the higher estimation of the oscillations.

Keywords: Balloon-multicopter, multicopter, lateral wind disturbance, hovering flight, friction joint.

NOMENCLATURE

BC	Ballooncopter
RS	Reference system
MC	Multicopter
BA	Balloon
PL	Payload
V_{xBA}, V_{yBA},V_{zBA}	The components of velocity of the balloon center in the ground reference system, m/s
V_{axBA}, V_{ayBA},V_{azBA}	The components of balloon aispeed, m/s
W_x, W_y	The x and y components of wind speed in ground reference system, m/s
X_{BA}, Z_{BA}	The coordinates of the center of mass of the balloon in the ground reference system, m
G_{BL}, $G_{T\text{-}PL}$	Ballast load and total payload, N
G_{SA}, G_{He}, G_{BA}	Weight of balloon shell, helium gas and the whole balloon, N
P_{ac}	Archimedes buoyancy force of the balloon, N
F_{EL}	Effective lift of the balloon, N
F_D	Aerodynamic force of the balloon, N
F_{Dx}, F_{Dy}	Projections of aerodynamic force in the X, Y directions relative to the ground reference system OXY, N
L_1	Length of suspension rod M'_1M_2, m
L_2	The radius of inertia of payload compartment relative to the joint, m
D	Diameter of sphere, m
S	Cross-sectional area of sphere, m^2

$L_1''=L_1+R$	Distance OM_2, m
γ_{0x}, γ_{0y}	Angles in X-axis and Y-axis of replacement M_1OM_1', rad
γ_{12}, γ_{11}	The angle from the vertical to the rod L_1, in the directions OX and OY. rad
γ_{22}, γ_{21}	The angle from the vertical to the line L_2, in the directions OX and OY. rad
H	Current altitude of the balloon center, m
F_{x0}, F_{y0}	Initial forces of multicopter to sustain desired altitude H_d and desired speed V_d, N
C_x, C_y	The coefficients of aerodynamic drag of balloon in the x-axis and y-axis
ρ_a, ρ_{He}	Density of air and helium, kg/m^3
M_{frx}, M_{fry}	friction moments in the hang joint of the paylod in the plans XM_2Z and YM_2Z respectly, Nm
K_{fr}	Coefficient of sliding friction
R	Radius of sliding surfaces relative to the rotation center of the joint, m
N	Normal reaction of a sliding surface, N
F_i	Inertia force, N
M_i	Inertia force moment, Nm

1. Introduction

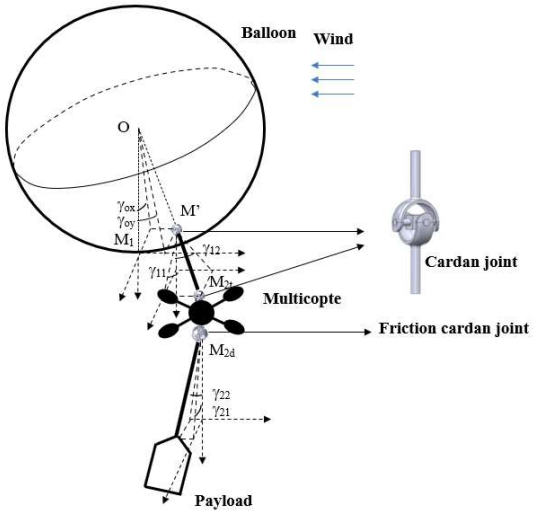

Figure 1. Overall layout of a balloncopter

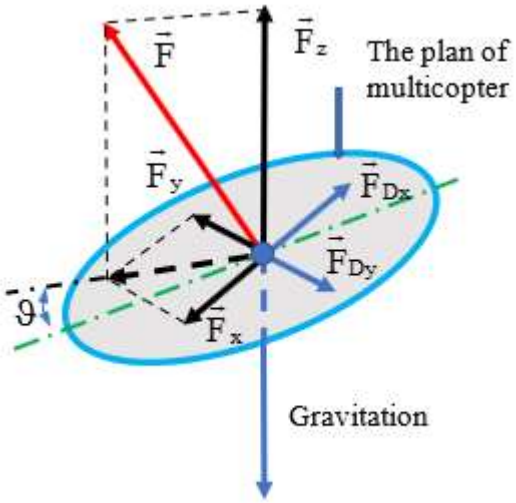

Figure 2. The components of thrust vector $\vec{\mathbf{F}}$: F_z (for weight balance) and F_x, F_y (for aerodynamic force balance $\vec{\mathbf{F}}_\mathbf{D}$)

Fig.1 shows the overall mechanical layout of a balloncopter [1] consisting of 3 main parts: the balloon, the multicopter and the payload. The combination of advantages of a balloon (long flight, high lift without losing energy, environmental friendliness) and those of a multicopter/ multirotor device (VTOL capability, easy to control both the attitude and the CG position when hovering and flying at low speed in windy conditions). This idea has been suggested for a long time four-rotor rotastat [2], however, the authors have proposed to rigidly attach the balloon (with payload compartment) to the multicopter [3], so it is still necessary to use high power rotors to tild the whole balloncopter with balloon and payload compartment for controlling the thrust vector. This article mentions that the balloncopter has a solution to assemble the multicopter with the balloon and the payload compartment due to 3 cardans forming a scheme of 2 seriesly hung pendulums (Fig. 1) that allows freely controll the plane of multicopter and consisquently the thrust vector F (Fig. 2) ...

The authorss suggested that the multicopter is conected with the balloon by a rigid rod. The rod has two cardan joints M'_1 and M_{2t} in its ends. The payload is hung to the multicopter also by a cardan

joint M_{2d}. Every joint of the three joints must have two degrees of fredom of rotation: pitch and roll. Such a construction provides the directional rotation (yaw) of the whole ballooncopter to hold the disêd flight path, particularly in the process of landing and moring at ground. In this case the yaw maneuvr and the maneuvrability is somewhat degreased, but it is not important for monitoring, tourism and many other aplications.

The lower joint M_{2d} to hang the payloađ is intentionally to have signìicant friction moment to damp the undesired oscillation of the payload that is important to monitoring.

The scheme of assembly allows to significantly reduce the necessary power of the rotors when tilting the thrust vector. This new assembly scheme requires balance and stability considerations when flying with and without wind turbulence. The full dynamic model of a new type of flight vehicle with such a complex mechanical layout is theoretically possible but it must be resolved step by step, at beginning we consider only longitudinal model, then consider the lateral model etc. The longitudinal motion was considered in the paper to be published in Aeronautical. Journal (UK) This paper deals with these problems in the scope of flight and hovering in presence of lateral wind.

The balloon's form is not necessarily spherical, but for the scope of this article we only consider the spherical balloon. and flying at low speed.

Coefficient of aerodynamic force was taken for the case of the sphere C_D=0.3 [4] at the number Re=3.10^6 and smooth surface.

Figure 2 introduces the known principle of controlling the movement of the multicopter center of mass by the thrust vector $\vec{\mathbf{F}}$: when tilting the vector $\vec{\mathbf{F}}$ to create the components $F_{x,y,z}$ to balance the appropriate forces : gravitation and aerodynamic drag caused by the airspeed. Thus, in order to control the ballooncopter, it is necessary to tilt the thrust vector $\vec{\mathbf{F}}$, that is, tilt the multicopter accordingly.

In this paper the fixed ground OgXZ and moving ground RS OXZ were accepted… Origin O of the RS is located at center of the balloon. OX axis is in the horizontal plane and toward the North, the OY axis is located also in the horizontal plane and perpendicular to the OX axis, the OZ axis is perpendicular to both said axises and directed downward perpendicularly to the ground plane composing a right tetraeder (fig. 6).

Now the static balance and the static stability of this ballooncopter scheme will be considered at a rectilinear horizontal uniform flight with lateral wind constantly acting in both the time and the space, then later the dynamic problem of flight of the ballooncopter will be conside with some additional assumptions to simplify the problem.

2. The static balance and the static stability and some qualitative analysis

The static equilibrium of the ballooncopter parts must be analyzed, and if the equilibrium is stable, that is, if the displacements of the points M_1', M_{2t} and M_{2d} in Fig.1, may not be too large.

Considering a rectilinear horizontal uniform flight to the North without wind, the forces acting on the ballooncopter must be balanced in the ground reference system along the Z-axis (vertical): and the X-axis (the North).

$$F_{EL} = G_{T-PL} + G_{MC} - F_z \tag{1}$$

$$F_x = -F_{Dx} \tag{2}$$

If constant lateral wind Wy acts on the ballooncopter that causes deviation of airspeed vector and the aerodynamic force vector F_D (Fig.3), To keep the fly path straight the forces acting along Y-axis also must be balanced:

$$F_y = -F_{Dy} \tag{3}$$

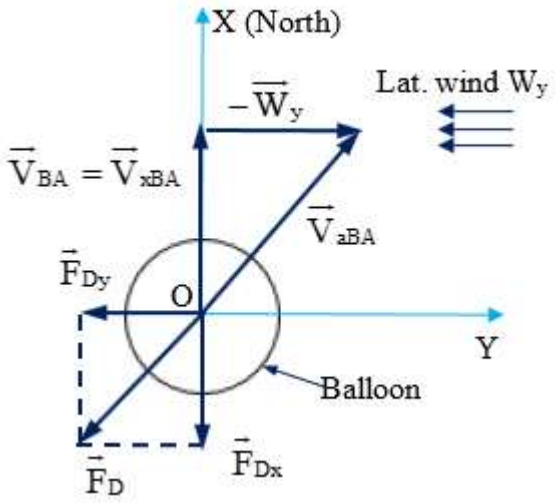

Figure 3. The vectors of airspeed, groundspeed of balloonicopter being acted by lateral wind. The balloonicopter fly path remains straight to the North due to the balance of the forces on y-axis.

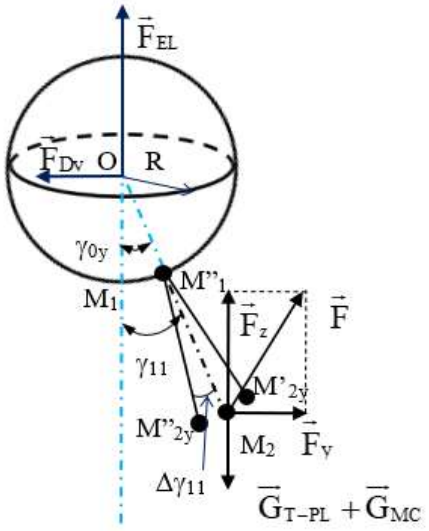

Figure 4. Static stability of the point M_2 (or of angle γ_{11})

According to the rule of three concurrent forces, the vector $\vec{\mathbf{T}}_\mathbf{1}$ – reaction of the suspension rod L_1 (line segment M'_1M_2) will have an action line that goes through the center point O, because the vectors $\vec{\mathbf{F}}_{\mathbf{Dx}}$ and $\vec{\mathbf{F}}_{\mathbf{EL}}$ both create a resulting force at the center O (due to symmetry of balloon). Hence, the angle γ_{0x} will be:

$$\gamma_{0x} = \text{arctg}\left(\frac{F_{Dx}}{F_{EL}}\right) \tag{4}$$

Similarly, the angle γ_{0y} will be:

$$\gamma_{0y} = \text{arctg}\left(\frac{F_{Dy}}{F_{EL}}\right) \tag{5}$$

On the other hand, the suspension rod L_1 must also lie in the radial direction through the center O of the sphere when the system is in equilibrium, i.e.:

$$\gamma_{0x} = \gamma_{12}\,,\ \gamma_{0y} = \gamma_{11} \tag{6}$$

For VASA-3M (that has total take-off weight 400kg and intends to flight with 3 people) at a rectilinear horizontal uniform flight with V=15 km/h and lateral wind W=15 km/h the angles are very small ($\gamma_{0x}=\gamma_{12}=3.1°$, $\gamma_{0y}=\gamma_{11}=3.1°$).

We will consider if this angular position of the pendulum L_1 is stable equilibrium. It is clear that when M_2 shifts to the position M_2' or M_2'' (or $\Delta\gamma_{11}$ appears) if always an unbalanced moment ΔM appears acting to liquidate the deviation $|\Delta\gamma_{11}| \to 0$ (figure 4):

Obviously that at rectilinear horizontal uniform flight the payload lies vertically and the angle $\gamma_{22}=0$ and it is a stable equilibrium.

The horizontal displacements a_x/a_y of the multicopter relative to the vertical line at rectilinear horizontal uniform flight without wind may be deduced from balance of the external moment relative to the point M_1' (assuming the angles to be small enough and ignoring the distance between the upper and

lower joints of multicopter, the upper joint M_{2t} and the lower joint M_{2d} are located in one and the same medium point M_2):

$$a_x = \frac{F_x}{K_1},\ a_y = \frac{F_y}{K_1} \tag{7}$$

$$K_1 = \frac{G_{T-PL} + G_{MC} - F_z}{L_1 + R} \tag{8}$$

That is, the pendulum mechanism L_1 acts almost like a spring with a stiffness K_1. When increasing the angles γ_{12} / γ_{11} the lever arm of the force ($G_{T\text{-}PL}$+G_{MC}-F_z) also increases, so that the appearing unbalanced moment will decrease the angles γ_{12} / γ_{11} and contrary. Thus, the equilibrium position of the angles γ_{12}= γ_{0x} and γ_{11}= γ_{0y} of the pendulum L_1 is a stable position. And the coefficient K_1 can be considered as the static stability of the balloon copter (similar to the distance from the center of mass to the aerodynamic center of a fixed-wing aircraft).

Note: force F_z<<($G_{T\text{-}PL}$+G_{MC}) so K_1 is generally >0. From the expression (6) for calculating the value of K_1, we see that "spring stiffness" (static stability of the balloon copter) is directly proportional to the weight of the hanging objects and inversely proportional to the total length of the suspension rod L_1 and the radius R.

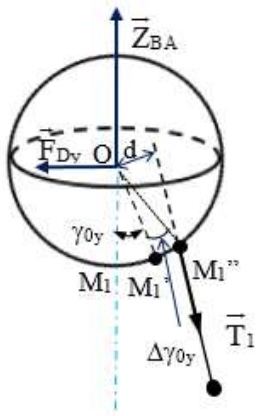

Figure 5. The static stability of the point M_1'

It is nescessary that the static stability of point M_1' (or angles γ_{0x} and γ_{0y}) also to be considered (fig. 5). If for example, a small deviation $\Delta\gamma_{0y}$ appears , it causes an unbalanced moment ΔM to recover the angle γ_{0y} or to liquidate the $\Delta\gamma_{0y}$. It means that the position of M_1' on the balloon envelope is also stable.

Of course, when multicopter motion has acceleration (e.g., while changing the vector $\vec{\mathbf{F}}$) there will be a pendulum effect of the payload hung to the multicopter at point M_2 by a joint and the angle ($\gamma_{21}\neq0$ or $\gamma_{22}\neq0$). When for example point M_2 has acceleration to the right ($\ddot{y}_{MC} > 0$) then mass $m_{T\text{-}PL}$ ($m_{T\text{-}PL}$=m_{PL}+$m_{S\text{-}PL}$+m_{BL}) that is about 350kg for VASA-3M will move to the left, creating a significant braking force to reduce acceleration $\ddot{y}_{MC}$, contrarily, when $\ddot{y}_{MC} < 0$ the same process happens but in the opposite direction. Through the above qualitative analysis, one can conclude that the balloon copter will be stable even when the motion has acceleration.

In short, qualitative analysis shows that the balloon copter can perform a stable flight with the action of lateral wind and to keep the fly path straight for example to the North, it's nescessary to create the force F_y= F_{Dy} by an automatic system of the multicopter.

3. Mathematical model of lateral motion of the balloncopter

To show that the system is dynamically stable system and to give a tool for computer aided engineering (CAE), the quantitative analysis will be done below for the dynamic model of the balloncopter in aperiodic and periodic disturbances of windy conditions with automatic flight control system. At first, one has to symplify the mechanical system accepting some assumptions.

3.1. The main assumptions

a) As mentioned, the dynamic problem will be divided into the problem without friction and the one with friction.In the second problem we'll consider the oscillations of the lower pendulum separately with oscillating hang joint when the maximal oscillations of the hang joint have been obtained from the first problem without friction. In this case one can obtain only the higher estimation of the oscillations, that is enough for practical purposes. Friction in the 2 joints M'_1 and the upper joint M_{2t} is neglected, the links of rotation masses are weightless and absolutely rigid. The third joint M_{2d} (to hang the payload) is considered without friction and with intentional friction.

In the problem with friction, static friction may be ignored because before the rotation is finally stopped the time interval that the angular speed is near to zero may be neglected.

As known, to create the friction moments M_{frx} and M_{fry} in the joint, one must create the friction force F_{fr} of sliding surfaces on a finite radius r, and the moments always act against the rotation, that is (if the static friction is ignored)

$$M_{frx} = -k_{fr} Nr \operatorname{sign}\left(\dot{\gamma}_{22}\right) \tag{9}$$

$$M_{fry} = -k_{fr} Nr \operatorname{sign}\left(\dot{\gamma}_{21}\right) \tag{10}$$

b) The attitude (pitch and roll) control system of the multicopter is assumed to be an ideal control system that means the attitude control of the multicopter is assumed to be performed instantaneously without errors. This assumption allows to neglect the rotation and the inertia moment of the multicopter in this dynamic problem. So the multicopter may be considered as a particle of mass m_{MC} with its translational motion without rotation.

c) The point M_1' is assumed always to be in a straight line with the points O and M_2 or we always have: $\gamma_{0x}=\gamma_{12}$ and $\gamma_{0y}=\gamma_{11}$.

d) The rotation of balloon around its center O may be ignored because its inẻtia moment relative to the center, and one may consider only its translational motion, so that the balloon may be considered as a particle of mass m_{BA}. The hung payload as a pendulum that will oscillate around the point M_2 may be considered as a pendulum comprising a particle of mass $m_{T\text{-}PL}$ hung by a rigid rod with length L_2 (radius of inertia of payload).

Thus, the whole balloncopter may be considered as a mechanical system consisting of 3 particles of mass m_{BA}, m_{MC} and m_{T-PL} connected by 2-DOF joints, in which the balloon, multicopter and payload are assumed to be considered as concentrated masses at points O, M_2, M_3 respectively.

e) When calculating the aerodynamic force acting to the sphere, the difference of the velocity field acting at different points of the sphere is ignored, the field is considered as a uniform field with the velocity value corresponding to the center O of the sphere.

f) Only the motion in the horizontal plane of the balloncopter is considered that is balloncopter has no vertical motion, that is asumpted the expesion (1) always is respected.

g) When considering the aerodynamic force, the focus is only done on the aerodynamic drag of the sphere $\vec{\mathbf{F}}_{\mathbf{D}}$, and the aerodynamic drag of the multicopter and of the payload compartment can be ignored because the cross-sectional areas of these parts is only a few percent of that of the balloon.

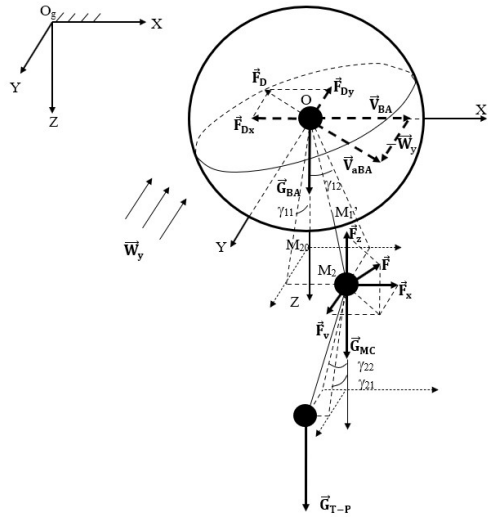

Figure 6. The dynamic model of the three-body mechanical system moving to the North and being acted by lateral wind

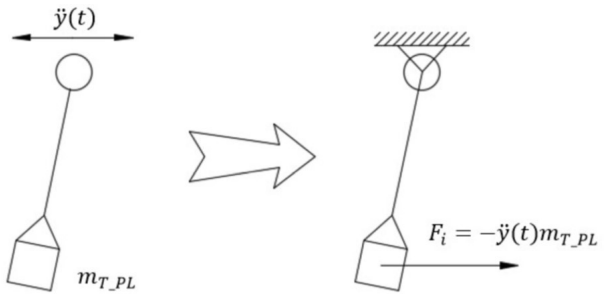

Figure 7. Converting the pendulum problem with moving hang joint to the problem with fixed hang joint

With the above said assumptions, we have a model of dynamics of the balloncopter in the lateral motion with friction -free joints was shown in fig.6. The fig.7 shows separately the problem of second pendulum (payload oscillations) with oscillating hang joint.The problem is converted to the classical pendulum problem with a fixed hang joint by inertia force Fi acting on the L_2 arm relative to the fixed hang joint as an external exciting factor . The vertical displacement of the hang joint may be neglected as a higher order small value. In this pendulum problem the friction moment (8) may be considered as well as an external factor.

Thus we'll consider two problems : the first one is a problem without friction and the second one is oscillation pendulum problem with friction. The problems are further presented in more details as follows.

3.2. The problem without friction

For the mechanical system shown at fig. 6 with constraints one can establish a system of differential equations of motion using the method of Lagrange equations type II [5] as following:
For the 6-DOF mechanical system the fully generalized coordinates were chosen as follows:

$q_1=X_{BA}$, $q_2=Y_{BA}$, $q_3=\gamma_{12}$, $q_4=\gamma_{11}$, $q_5=\gamma_{22}$, $q_6=\gamma_{21}$ ($\gamma_{11},\gamma_{12},\gamma_{21},\gamma_{22}>0$ when turning counterclockwise).

Action forces acting on the system: P_{ac}, G_{KC}, G_{MC}, G_{tong_TCI}, F_x, F_y, F_z, F_{Dx}, F_{Dy}.

Where: $G_{BA} = m_{BA}g$, $G_{MC} = m_{MC}g$, $G_{T-PL} = m_{T-PL}g$

$$F_{Dx} = \text{sign}\left(V_{xBA} - W_x\right)0.5C_x\rho_a S\left(V_{xBA} - W_x\right)^2 \tag{11}$$

$$F_{Dy} = \text{sign}\left(V_{yBA} - W_y\right)0.5C_y\rho_a S\left(V_{yBA} - W_y\right)^2 \tag{12}$$

Kinetic energy: $T = T_{BA} + T_{MC} + T_{PL}$

$$T_{BA}=\frac{1}{2}m_{BA}\left(\dot{X}_{BA}^2+\dot{Z}_{BA}^2\right);T_{MC}=\frac{1}{2}m_{MC}\left(\dot{X}_{MC}^2+\dot{Y}_{MC}^2+\dot{Z}_{MC}^2\right);T_{PL}=\frac{1}{2}m_{T-PL}\left(\dot{X}_{PL}^2+\dot{Y}_{PL}^2+\dot{Z}_{PL}^2\right) \quad (13)$$

$$\begin{cases} X_{M_2}=X_{MC}=X_{BA}+L_1^{'}\dfrac{tg\gamma_{12}}{\sqrt{1+tg^2\gamma_{12}+tg^2\gamma_{11}}} \\ Y_{M_2}=Y_{MC}=Y_{BA}+L_1^{'}\dfrac{tg\gamma_{11}}{\sqrt{1+tg^2\gamma_{12}+tg^2\gamma_{11}}} \\ Z_{M_2}=Z_{MC}=H_0-L_1^{'}\dfrac{1}{\sqrt{1+tg^2\gamma_{12}+tg^2\gamma_{11}}} \end{cases};\begin{cases} X_{PL}=X_{MC}+L_2\dfrac{tg\gamma_{22}}{\sqrt{1+tg^2\gamma_{22}+tg^2\gamma_{21}}} \\ Y_{PL}=Y_{MC}+L_2\dfrac{tg\gamma_{21}}{\sqrt{1+tg^2\gamma_{22}+tg^2\gamma_{21}}} \\ Z_{PL}=Z_{MC}-L_2\dfrac{1}{\sqrt{1+tg^2\gamma_{22}+tg^2\gamma_{21}}} \end{cases} \quad (14)$$

Generalized force: Total power of the active forces

$$\sum CS=-F_{Dx}\dot{X}_{BA}-F_{Dy}\dot{Y}_{BA}+F_x\dot{X}_{MC}+F_y\dot{Y}_{MC}+\left(F_z+G_{MC}\right)\dot{Z}_{MC}+G_{tong-TCl}\dot{Z}_{PL} \quad (15)$$

The partial derivatives of the generalized forces to the corresponding generalized coordinates:

$$Q_i=\frac{\partial\sum CS}{\partial\dot{q}_i},\ i=1\ldots6 \quad (16)$$

Substitute the above expressions into the Lagrange equations of type II

$$\frac{d}{dt}\left(\frac{\partial T}{\partial\dot{q}_i}\right)-\frac{\partial T}{\partial q_i}=Q_i,\ i=1\ldots6 \quad (17)$$

Then one can set up a system of differential equations for the motion of the system. The process of loading input data, calculating the above formulas and solving the system (by numerical method) is done in MAPLE. Thus, it will be possible to build a software to calculate and determine the motion parameters of the mechanical system, this software needs to be tested qualitatively and quantitatively to confirm the reliability, which will be presented in the following paragraph.

3.3. The problem with friction

As mentioned the problem of the whole 3-body mechanical system gives the accelleration $\ddot{y}(t)$ that will be as input data for the oscillation pendulum problem in the planes M_2XZ and M_2YZ (fig.7, shown in the plane M_2YZ) acting as inertia force $F_{iy}=-\ddot{y}(t)m_{T-PL}$ on the arm L_2 and creating moment M_{iy}. One can establish an ordinary differential equation for the classical pendulum relative to angle γ_{21} with external moments $M_{iy}=F_{iy}.L_2$, friction moment M_{fry} (8) and gravity moment $gm_{T\text{-}PL}L_2\gamma_{21}$ (The diference bettween CG and center of inertia is neglected and the angle γ_{21} was found as small angle):

$$-L_2\ddot{y}(t)m_{T-PL}-k_{fry}Nr\,sign\left(\dot{\gamma}_{21}\right)-gm_{T-PL}L_2\gamma_{21}=L_2^2m_{T-PL}\ddot{\gamma}_{21} \quad (18)$$

To overcome the dificulty in numerical solution in MAPLE the function sign(x) discontinued at x=0 is approximated by a continued function $\frac{2}{\pi}arctg(10x)$.

3.4. Calculations and discussions

The motion dynamics of a hypothetical balloncopter KCTT-20 was investigated with input data and initial data as follows.

3.4.2. Input data

D=5m; H_0=203.5m; V_{0xBA}=4m/s (if rectilinear flight); V_{0xBA}=0 (if hovering); V_{0zBA}=0.

$C_x=C_y=0.3$; $g=9.81 m/s^2$; $L_1=1m$; $L_2=1.5m$. $m_{PL}=20kg$; $m_{SBA}=16kg$; $m_{MC}=14kg$; $m_{S-PL}=4kg$; $m_{BL}=4kg$ (ballast load); $\rho_a=1.16 kg/m^3$; $\rho_{He}=0.16\ kg/m^3$. $R=D/2=2,5m$; $S=\pi R^2=19.62m^2$; $VOL=(4\pi R^3)/3=65.4m^3$; $m_{He}=\rho_{He}VOL=10.5kg$; $m_{BA}=m_{SBA}+m_{He}=26.5kg$; $m_{T-PL}=m_{PL}+m_{S-PL}+m_{BL}$; $m_T=m_{BA}+m_{MC}+m_{T-PL}$. $P_{ac}=VOL\rho_a g$.

The case with friction: Coefficient of sliding friction $K_{fr}=0.94$, aluminium/ aluminium [6], normal reaction of sliding surfaces $N=g.m_{T-PL}= 196N$, the radius of sliding surfaces $r=0.05$ m

3.4.3. Initial conditions

a) Rectilinear flight: $F_{Dx0} = -0.5C_x\rho_a SV_{ax}^2$; $F_{Dx0} = -0.5C_x\rho_a SV_{ay}^2$; $F_x = F_{Dx0}$; $F_y = F_{Dy0}$.

$\gamma_{210} = \text{acrtag}\left(\frac{F_{Dx0}}{F_{EL}}\right)$; $\gamma_{110} = \text{acrtag}\left(\frac{F_{Dy0}}{F_{EL}}\right)$; $\gamma_{210}=0$; $\gamma_{220}=0$.

b) Hovering: $F_{Dx0}=0$; $F_{Dy0}=0$; $F_x=F_{Dx0}$; $F_y=F_{Dy0}$; $\gamma_{120}=0$; $\gamma_{220}=0$; $\gamma_0=0$.

3.4.4. Verification of the software

We can test qualitatively by increasing or decreasing some parameters and also quantitatively for a few particular cases with known solutions in advance. For example, the authors tested qualitatively as follows: changing tailwind/headwind speed, air density, diameter of the balloon, control force of the multicopter, etc. And all simulation results were changed in appropriate directions. Quantitative testing for some particular cases such as: test of asymptotic cases, for example for $C_x\to 0$, L_1, $L_2\to\infty$, then the results are also asymptotically approach to the known limits.

It is a fact that most of the results of numerical solutions can only be *tested qualitatively* and tested *quantitatively in a few special cases.* Therefore, confirming the general correctness of mathematical model and software often requires physical tests that are complicated and sometimes dangerous, which are sometimes more difficult and expensive than the development of mathematical model and software.

In this problem, in addition to the qualitative test, we can use the change in the kinetic energy of the system and the work of the external forces to quantitatively check the calculation results. Specifically, according to theoretical mechanics, there is the kinetic energy variation theorem of a mechanical system: *"The time derivative of the kinetic energy of a mechanical system is equal to the sum of the powers of the internal forces and external forces acting on the system"*. Applying to the dynamic model, according to this theorem (the work of the internal force is zero), we have the following expression:

$$\frac{dT}{dt} = -F_{Dx}\dot{X}_{BA} - F_{Dy}\dot{Y}_{BA} + F_x\dot{X}_{MC} + F_y\dot{Y}_{MC} + \left(F_z + G_{MC}\right)\dot{Z}_{MC} + G_{tong-TCI}\dot{Z}_{PL} \tag{19}$$

Performing the calculation to check the formula (19) in MAPLE we see that this formula is satisfied at every time moment.

3.4.3. Some calculation results and discussion

a) The case of a *rectilinear* horizontal uniform *flight* to the North with constant Eastern wind W_y=-4m/s, encountering latėal step disturbance $\begin{cases} W_y = -4\ m/s \text{ when } t < 6s \\ W_y = -7.6\ m/s \text{ when } t > 6s \end{cases}$

The maximal wind= 7.6 m/s (27.4 km/h) was taken from JAR-VLA [7]. The simple autopilod was used

$$F_y = F_{y0} + K_p y + K_d V_y \tag{20}$$

Where K_p=-20 N/m and K_d= -10 N/(m/s). One can see (fig. 8) there is an significant static error, that isn't important in this case and may be liquidated by addition of an intergral member .

We have some calculation results as follows (fig. 8, 9, 10,11a):

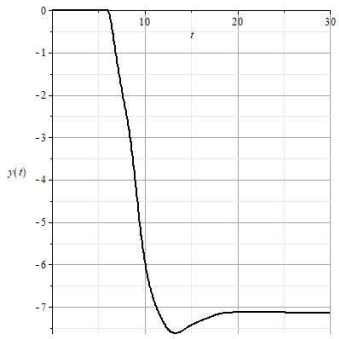

Figure 8. The deviation of the balloon copter y(t) from the OX -axis when encountering lateral wind, step disturbance

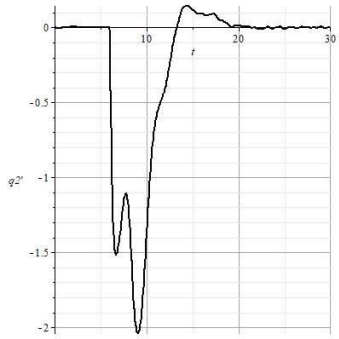

Figure 9. The deviation speed of the balloon copter $V_y(t)$ from the OX -axis when encountering lateral wind, step disturbance

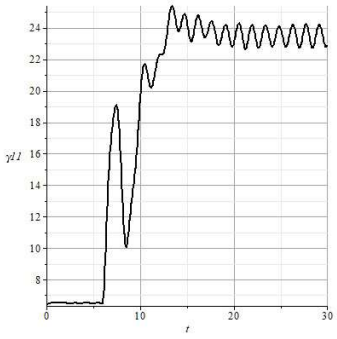

Figure 10. The oscillation angle of the multicopter $\gamma_{11}(t)$ when encountering lateral wind, step disturbance

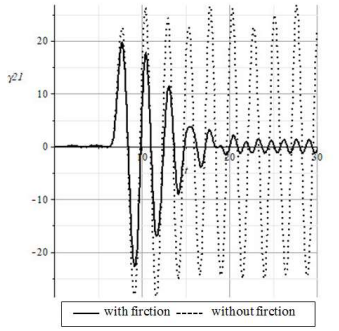

Figure 11. The oscillation angle of the payload $\gamma_{21}(t)$ when encountering lateral wind step disturbance (a) and when encountering wind step disturbance (b)

b) The case of *hovering* without wind and encountring step wind disturbance

$$\begin{cases} W_y = 0 \text{ when } t < 6s \\ W_y = -7.6\ m/s \text{ when } t > 6s \end{cases}$$

We have some results of calculating the motion parameters of the balloon copter as follows (fig. 12,13,14, 15):

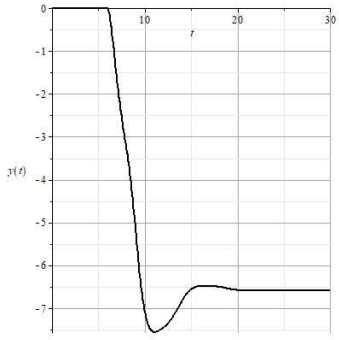

Figure 12. The deviation of the balloon copter y(t) from the OX -axis when encountering wind step disturbance

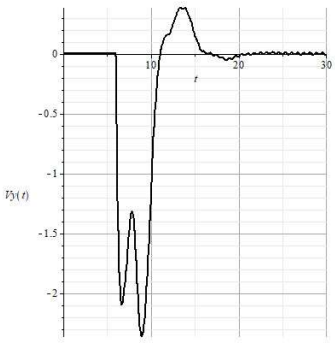

Figure 13. The deviation speed of the balloon copter $V_y(t)$ from the OX -axis when encountering wind step disturbance

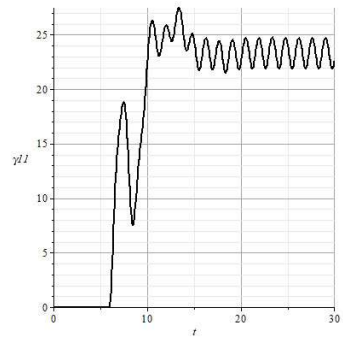

Figure 14. The oscillation angle of the multicopter $\gamma_{11}(t)$ when encountering wind step disturbance

One can see, as well as in previous case, the static error of y(t) (fig.12), when used the same autopilot (20). The fig.15 shows that the undesired oscillations of the payload can be damped by the joint with enough friction moment.

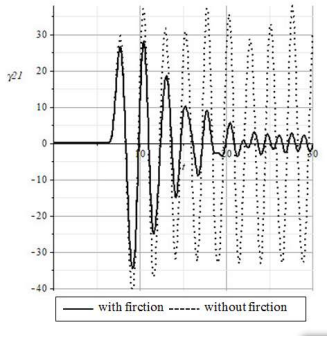

Figure 15. The oscillation angle of the payload $\gamma_{21}(t)$ when encountering lateral wind step disturbance

4. Conclusion

This article deals with the ballooncopter with special assembly solution to hang the multicopter with the balloon and payload compartment according to the scheme of two pendulums suspended in series. This new assembly scheme has been considered for balance and stability in the scope of the flight and the hovering in the wind disturbances. The lateral motion of the ballooncopter is modeled by a 3-body, 6-degree-of-freedom system, and the motion law of the system is determined by the method of Lagrange II equations, the calculation is done in MAPLE. The software is accurately tested to determine its reliability when used as a design aid tool. The calculation results confirmed for a hypothetical ballooncopters its flight dynamic stability in wind disturbance, including hovering flight. The cardan joint for the payload must has intentionally friction enough to damp the oscillations of the payload that is necessary to improve the infformations given by the payload in monitoring misions. In this case the authors suggest to obtain the higher estimation of the oscillations by assumption that there is no revers action to the whole 3-body mechanical system from the damped payload oscillations.

References

[1] Nguyễn Đức Cương, Trần Duy Duyên và nnk - Mô tả sáng chế, "Phương tiện bay trực thăng nhẹ hơn không khí" Công báo Sở hữu công nghiệp số tháng 9/2021, Cục Sở hữu trí tuệ Việt Nam (Invention description published by Vietnam Intellectual Property Office).

[2] Khoury, Gabriel Alexander (Editor), *Airship Technology*, Cambridge Aerospace Series, (2012).

[3] Umberto Papa et al. Conceptual Design of a Small Hybrid Unmanned Aircraft System, *Journal of Advanced Transportation*, Vol 2017, 10 p.

[4]https://en.wikipedia.org/wiki/Drag_coefficient#/media/File:Drag_coefficient_on_a_sphere_vs._Reynolds_number_-_main_trends.svg

[5] Đỗ Sanh, *Cơ học tập 2*, NXB Giáo dục, Hà Nội, (1998).

[6] https://himya.ru/koefficient-treniya-tablicy-elektronnogo-spravochnika-po-ximii-soderzhashhie-koefficient-treniya.html

[7] Joint Aviation Requirements—Very Light Aircraft (JAR-VLA. pdf, Apr 26, 1990).